Letters

An Efficient and Reliable Solid-State Circuit Breaker Based on Mixture Device

Xiaorui Xu, *Student Member, IEEE*, Wanjun Chen, *Senior Member, IEEE*, Chao Liu, Ruize Sun, *Member, IEEE*, Zhaoji Li, *Member, IEEE*, and Bo Zhang, *Senior Member, IEEE*

***Abstract*—In this letter, a novel solid-state circuit breaker (SSCB) based on mixture device (MD-SSCB) is proposed for dc distribution systems. The proposed MD-SSCB can actively interrupt faults without introducing additional thyristor, charging power supply, and charging strategies. Besides, the interruption capability of the MD-SSCB is not affected by the parameters of the outer circuit. As a result, the MD-SSCB has advantages of compact structure, economic design, high efficiency, and high reliability. Moreover, the MD-SSCB can turn OFF its thyristors without reverse voltage stress, which eliminates the severe reverse overvoltage problem in the fault-interrupting process, and hence further enhances the reliability of the breaker. Detailed operation principle and design guidelines of the MD-SSCB are discussed through mathematical modeling. The feasibility of the proposed breaker is validated by experimental results.**

***Index Terms*—DC circuit breaker, power system protection, solid-state circuit design, thyristor.**

I. Introduction

DIRECT current (dc) distribution systems have been developed increasingly in recent years because of its unique characteristics [1], [2]. However, due to the high fault current rising rate and the lack of natural current zero-crossing point, dc distribution systems face more difficult fault breaking problems than ac systems. Therefore, dc circuit breakers with fast reaction and reliable breaking capability are required.

Differing from ac systems, using traditional mechanical circuit breakers (MCBs) to protect dc distribution systems will cause arc erosion, resulting in a high maintenance cost [3]. Hybrid circuit breakers (HCBs) are an acceptable solution, and have been applied in some high-voltage dc (HVdc) systems, such as Zhang Bei 500 kV dc grid [4]. Nevertheless, mechanical ultrafast disconnectors (UFDs) adopted in HCBs need a long contact separation time (several microseconds [5]), slowing the breaking speed and increasing the fault current that needs to be interrupted. Moreover, UFDs also increase the weight, volume, and investment of HCBs.

Compared with MCBs and HCBs, solid-state circuit breakers (SSCBs) based on semiconductor devices have advantages of faster reaction, simpler control, and more compact volume. IGBT-based SSCBs have been proposed and successfully applied to dc distribution systems [6]. However, these breakers suffer from large conduction losses and high configuration cost. Recently, SSCBs based on wide-band gap semiconductor devices (e.g., SiC MOSFETs and GaN HEMTs) have also been proposed, which have advantage of high power density. But now, the high device cost and reliability concerns are the main obstacles that need to be overcome [7].

Compared with full-controlled devices, half-controlled devices (e.g., thyristors) feature smaller conduction losses, smaller volume, and lower costs, thus being attractive in dc system protection. However, thyristors suffer from poor hard turn-OFF capability, which makes reliable turn OFF of thyristors a challenging task. Integrated gate-commutated thyristors (IGCTs) can commutate the current from the cathode to the gate, which forces the device to exit latch-up mode, and thus turns OFF the device [8]. However, the specially designed gate driver significantly increases costs and volume of IGCTs. Another method is to create current zero-crossing point for thyristors by introducing the commutating path in the circuit design, which is called the commutation-forced turn-OFF principle. Based on this principle, a thyristor-based SSCB was proposed to interrupt fault dc current in [9]. However, this breaker needs additional charging power supply and charging strategies to precharge its commutating capacitor, which increases the control complexity and investment of the breaker. The breakers that can charge their commutating capacitor through dc sources were proposed in [10] and [11], but their topologies and control strategies are too complicated to achieve compact integration and intelligent control. The ZSCB and the ΓSCB with simpler topology were also designed in [12] and [3], respectively. Unfortunately, the interruption capability of these breakers is affected by the parameters of the outer circuit. Hence, they may malfunction under high-resistance faults or the influence of system parasitic inductance. Besides, these breakers can only be passively turned OFF in some special cases. This problem can be solved by introducing additional manual tripping thyristors [3], but at expense of higher costs and larger

Manuscript received January 17, 2021; revised February 15, 2021 and March 8, 2021; accepted March 16, 2021. Date of publication March 18, 2021; date of current version June 1, 2021. This work was supported in part by the National Natural Science Foundation of China under Grant 51877030 and in part by the Stable Support Project under Grant JCKY201924C002. (Corresponding authors: *Wanjun Chen, Xiaorui Xu*.)

The authors are with the State Key Laboratory of Electronic Thin Films and Integrated Devices, University of Electronic Science and Technology of China, Chengdu 610054, China (e-mail: 81676902@qq.com; wjchen@uestc.edu.cn; 893516228@qq.com; rzsun@uestc.edu.cn; zjli@uestc.edu.cn; zhangbo@uestc.edu.cn).

Color versions of one or more figures in this article are available at https://doi.org/10.1109/TPEL.2021.3067316.

Digital Object Identifier 10.1109/TPEL.2021.3067316

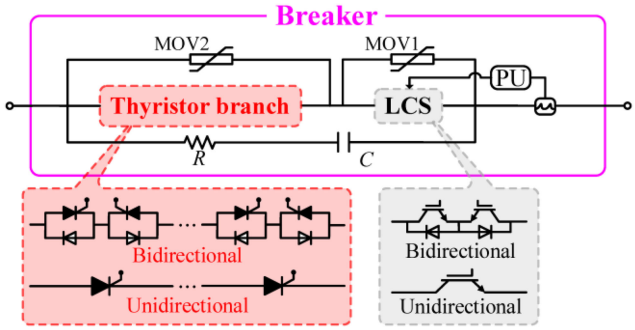

Fig. 1. Topology of the proposed MD-SSCB.

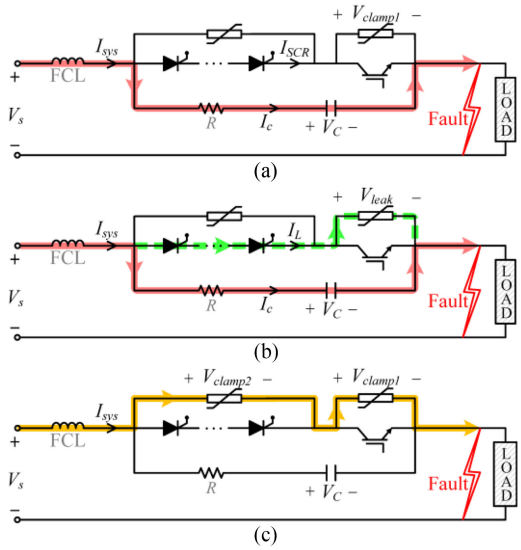

Fig. 2. Fault modeling of the MD-SSCB at (a) the current commutation stage, (b) the thyristor recovery stage, and (c) the energy releasing stage.

volume, especially when applied to medium-voltage dc (MVdc) and HVdc system protection. More importantly, the existing thyristor-based SSCBs require reverse voltage stress to reversely recover their thyristors, thus ensuring successful turn OFF of their thyristors. However, the reverse recovery process (RRP) of the thyristor will induce a severe overvoltage problem, which will cause aging and damages of power devices, and hence degrades the reliability of breakers [13].

In order to overcome those problems, this letter proposes a novel SSCB based on mixture device (MD-SSCB), which is mainly used for MVdc and HVdc distribution system protection. The MD-SSCB can actively interrupt faults without the additional thyristor, charging power supply and strategies. Besides, the interruption capability of the MD-SSCB is not influenced by the parameters of the outer circuit. Consequently, the MD-SSCB can provide simpler structure, lower costs, higher efficiency, and higher reliability than the existing breakers. Moreover, the MD-SSCB can turn OFF its thyristors without reverse voltage stress. This eliminates the severe reverse overvoltage problem during the fault interrupting process, which further enhances the reliability of the breaker.

II. Analysis and Design Guidelines of MD-SSCB

A. Topology Introduction

Fig. 1 shows the topology of the proposed MD-SSCB, which can be divided into three paths: 1) the main current path (MP); 2) the commutating path (CP); 3) the energy releasing path (EP). The MP is composed of the thyristor branch, the line commutation switch (LCS), and the protecting unit (PU). The thyristor branch is a set of thyristors in series connection. Here, IGBTs are used as an example to form the LCS and other full-controlled devices are also acceptable. The CP is made up of a resistor (R), and a commutating capacitor (C). If necessary, diodes can also be added in the CP to form the *R-C-D* circuit, which can reduce the discharge current of C, thus avoiding possible damages to power devices and suppressing oscillations [14]. The EP consists of metal oxide varistors (MOVs). Since both bidirectional and unidirectional topologies have the same operating principle, the unidirectional one is taken as an example in the following text.

In the normal ON-state, the system rated current (I_{rate}) flows through the MP to power the load. Owning to the low conduction losses of the thyristor branch, the MD-SSCB can achieve high power efficiency. In the OFF state, the most of the system voltage (V_s) is supported by the thyristor branch. As a result, only a few expensive IGBTs are needed, and hence the costs of the MD-SSCB can be significantly reduced.

B. Fault-Interrupting Principle and Modeling

When a fault occurs, the PU will send a turn-OFF command to IGBT once the fault current exceeds the preset threshold (I_T) of the PU. Then, the MD-SSCB operates in fault-interrupting process, which can be divided into three stages shown in Fig. 2.

1) Stage 1: Current Commutation: After the IGBT is turned OFF, the fault current will be conducted by the MOV1 connected in parallel with the IGBT. Therefore, the voltage across the MOV1 suddenly increases to the clamping voltage (V_{clamp1}), as shown in Fig. 2(a). This voltage step change will generate a large current (I_c) in the CP to charge C, thus causing most of the system current (I_{sys}) to flow into the CP. Therefore, the thyristor branch current (I_{SCR}) will drop to zero, forcing the thyristors to exit latch-up mode.

Because the voltage is suddenly changed in this stage, I_{sys} retains I_T. By neglecting the ON-state voltage drops of the switches, one can be obtained by KVL

$$V_{clamp1} = I_c\, R + \frac{1}{C}\int I_c dt. \tag{1}$$

As a result, the maximum I_c in this stage can be expressed as

$$I_c = \frac{V_{clamp1}}{R}. \tag{2}$$

Then, I_{SCR} can be derived according to KCL

$$I_{SCR} = I_T - \frac{V_{clamp1}}{R}. \tag{3}$$

To make I_{SCR} drop to zero, R should meet

$$R \le \frac{V_{clamp1}}{\alpha I_T} \tag{4}$$

where α is an attenuation coefficient related to the system equivalent series inductance. For the safety, $\alpha = 2$ is suggested. Besides, because *R* will capture a high pulse current at this stage, the required peak voltage (V_{R_peak}) of *R* should meet

$$V_{R\_peak} \geq 2I_T R. \tag{5}$$

2) Stage 2: Thyristor Recovery: As shown in Fig. 2(b), after I_{SCR} drops to zero, V_s still charges *C*, which makes V_c keep increasing. In the MP, the increased voltage is supported by the MOV1, which makes the MOV1 work in the leakage region and conduct a leakage current. If the leakage current is less than the thyristor latching current (I_L), the thyristor branch will extract the excess carriers stored in the thyristors to support the leakage current. Since little voltage is borne by the thyristor branch at this stage, it can be concluded that the thyristors are recovered at quasi-zero voltage, which avoids the severe reverse overvoltage problem that jeopardizes the reliable operation of the breakers [13], and thus enhances the reliability of the dc system.

For a reliable turn-OFF of the thyristor branch, the thyristor recovery duration ($\triangle t$) is required to be longer than the intrinsic recovery time of the thyristors (t_r). Due to the presence of the fault current limiter (FCL), I_c can be assumed to retain I_T at this stage. Thus, $\triangle t$ can be calculated according to (1)

$$\Delta t = \frac{2C}{I_T}\left[V_{leak}\left(I_L\right) - I_T R\right]. \tag{6}$$

In order to turn OFF the thyristor branch, *C* should meet

$$C > \frac{I_T t_r}{2\left[V_{leak}\left(I_L\right) - I_T R\right]} \tag{7}$$

where $V_{leak}(I_L)$ is the leakage voltage when the MOV1 conducts a leakage current of I_L. Typically, $V_{leak}(I_L)$ is slightly smaller than V_{clamp1}.

3) Stage 3: Energy Releasing: After the thyristor branch is successfully turned OFF, the residual energy stored in the dc system inductance (L_{sys}) will be released through the EP, as shown in Fig. 2(c). This will lead to voltage overshoots in the thyristor branch, the IGBT and *C*. A generally accepted peak clamping voltage range of MOV (V_{clamp}) can be given by [15]

$$1.5 \text{ p.u.} < V_{\text{clamp}} < 2.5 \text{ p.u.} \tag{8}$$

where 1 p.u. is the continuous dc voltage of MOV. For the safety, the blocking voltage (*BV*) of the thyristor branch, the IGBT and *C* should meet

$$\begin{cases} BV_{IGBT} \geq V_{clamp1} \\ BV_{SCR} \geq V_{clamp2} \\ BV_C \geq V_{clamp1} + V_{clamp2} \end{cases} \tag{9}$$

where BV_{IGBT}, BV_{SCR}, and BV_C are the breakdown voltages of the IGBT, the thyristor branch and *C*, respectively. Besides, assuming that the total clamping voltage of the MOVs is twice V_s, the required energy absorption capability of the MOV (E_{MOV}) can be obtained by integrating the power across the MOV as

$$E_{MOV} \geq \int I_{MOV} V_{clamp} dt \approx \frac{{I_T}^2 L_{sys} V_{clamp}}{2V_s} \tag{10}$$

where I_{MOV} is the MOV current. Moreover, the MOV lifetime is also crucial because it affects the lifetime of the breaker. The MOV lifetime will decrease with the increase of voltage/temperature stress, surge current, and impulse duration. As a result, the mean time to failure (MTTF) and the repetitive surge capability of the MOV must be considered when designing and maintaining the MD-SSCB.

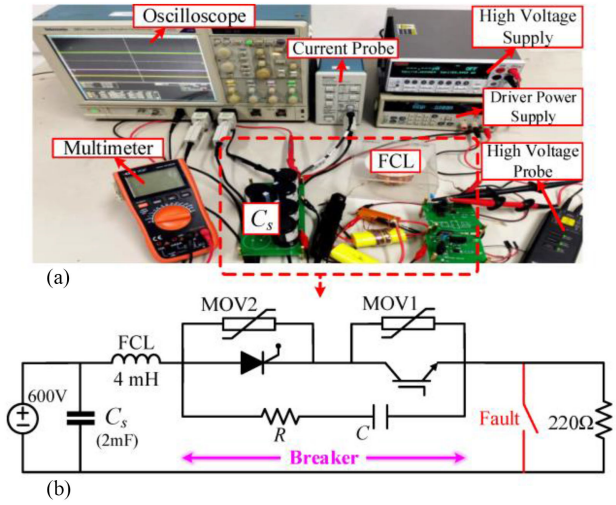

Fig. 3. (a) Photograph and (b) circuit diagram of the experimental setup.

C. Design Guidelines

Based on the established model, the MD-SSCB can be designed with the following guidelines.

1) Determine the MOVs and the preset threshold I_T according to (10) and the overload capacity of dc systems, respectively.
2) Select thyristors and IGBTs according to (9) and the current rating of dc systems (i.e., $BV \geq V_{clamp}$, $I_{T(AV)M} \geq I_{rate}$). Besides, the current turn-OFF capability of IGBTs is also required to be larger than I_T.
3) Choose R referring to (4) and (5), and choose C referring to (7) and (9). Since the model is established under ideal conditions, suitable margins should be reserved when determining the circuit components.

III. Breaker Verification

A. Experimental Results

Based on the design guidelines, a scaled-down experimental prototype is built to verify the feasibility of the MD-SSCB, as shown in Fig. 3. In the experiment, dc voltage and I_T are set to 600 V and 45 A, respectively. A 1.2 kV thyristor with I_L of 700 mA and t_r of 15 μs, and a 45 V MOV1 with V_{clamp1} of 100 V and $V_{leak}(I_L)$ of 71 V are chosen. Hence, a 250 V IGBT (*FGD3325G2F085*) is selected. Besides, *R* of 0.8 Ω and *C* of 10 μF can be determined according to the design guidelines.

The fault-interrupting waveforms of the MD-SSCB are presented in Fig. 4. It can be seen that after the fault occurs at $t = 0$, the system current (I_{sys}) increases and reaches I_T fast. Then, the IGBT is turned OFF, triggering the interruption process of the MD-SSCB. As a result, the thyristor is turned OFF to isolate the fault and support the major system voltage. Finally,

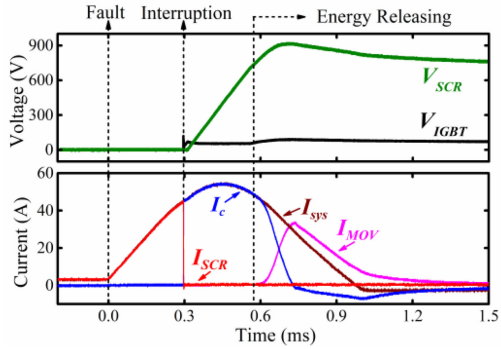

Fig. 4. Measured fault-interrupting waveforms of the MD-SSCB.

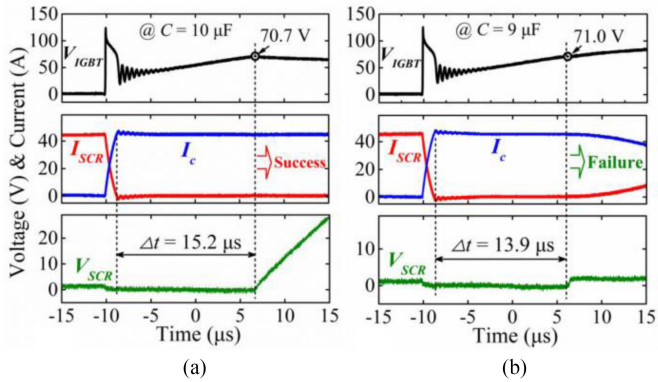

Fig. 5. Measured waveforms during the thyristor recovery stage at (a) $C = 10$ μF, and (b) $C = 9$ μF.

the residual energy is released through the MOV1 and MOV2, causing voltage overshoots at the thyristor and IGBT.

Fig. 5 shows the detailed waveforms during the thyristor recovery stage. As analyzed above, a reliable turn-OFF of the thyristor must satisfy $\triangle t > t_r$. Consequently, when C of 10 μF is chosen in Fig. 5(a), the MD-SSCB has $\triangle t$ of 15.2 μs (larger than t_r), which turns OFF the thyristor successfully. However, when C is reduced to 9 μF in Fig. 5(b), the breaker is failed to interrupt the fault because $\triangle t$ is smaller than t_r at this case. Fig. 5(a) also demonstrates that for the MD-SSCB, the thyristor can be successfully turned OFF after completing the recovery process at quasi-zero voltage, which avoids the severe reverse overvoltage problem [13], and thus enhances the reliability of the MD-SSCB. Moreover, a good agreement between the experimental results and the theoretical results is achieved, which verifies the feasibility of the MD-SSCB and the accuracy of the design guidelines.

B. Practical Evaluation

In this part, a MD-SSCB that is suitable for a 25-kV/2-kA dc distribution system is established and modeled in MATLAB/Simulink. According to the design guidelines, the thyristor branch consists of seven 5.2 kV thyristors (*T1451N*) in series. The LCS consists of four 6.5 kV IGBTs (*5SNA 0500J650300*) in parallel. Detailed parameters are listed in Table I. MOVs

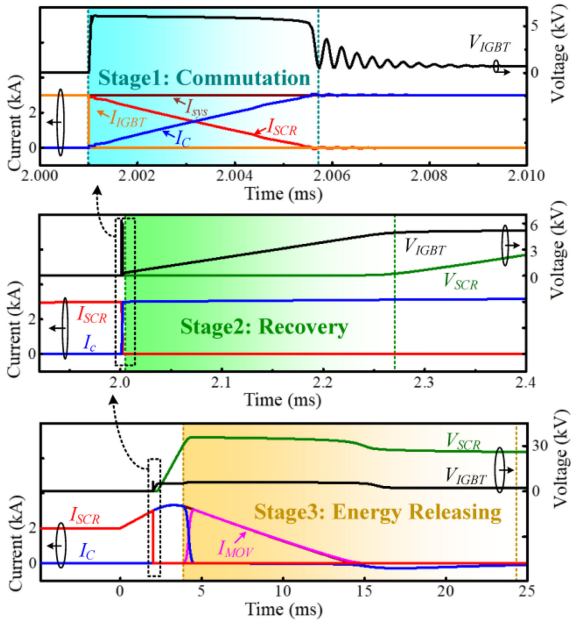

Fig. 6. Simulation waveforms of the 25-kV/2-kA MD-SSCB.

TABLE I
PARAMETERS OF THE MD-SSCB FOR 25-KV/2-KA SYSTEM

V_s	I_{rate}	I_T	V_{clamp1}	$V_{leak}(I_L)$	I_L	t_r
25 kV	2 kA	3 kA	6.2 kV	5.1 kV	1.5 A	250 μs

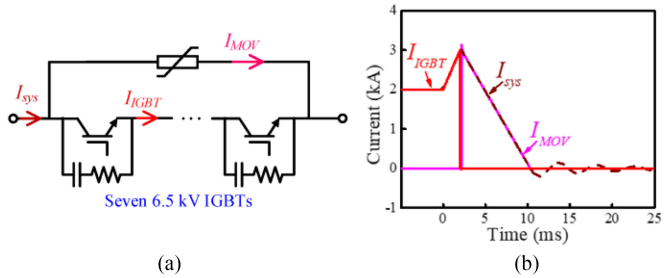

Fig. 7. (a) Topology, and (b) interrupting waveforms of the IGBT-based SSCB.

refer to *V202CA60*. Hence, R of 0.1 Ω and C of 90 μF can be determined according to (4) and (7), respectively. The simulation results are given in Fig. 6, which shows that after a fault occurs at $t = 0$, the MD-SSCB operates in the current commutation, thyristor recovery, and energy releasing stages in sequence, and finally interrupts the fault successfully. This further proves the practical value of the MD-SSCB.

In addition to the MD-SSCB, the IGBT-based SSCB [6] and the HCB [1] can also be used in a 25-kV/2-kA dc distribution system. As a result, the fault-interrupting performance of these two breakers are further simulated. Both the topologies and results of the IGBT-based SSCB and the HCB are shown in Figs. 7 and 8, respectively. Here, IGBT (*5SNA0500J650300*) and UFD ($LW36SF_6$) are selected. Each IGBT is connected in parallel with a snubber circuit (0.1-Ω energy dissipating resistor and 30-μF bypass capacitor) to balance the dynamic

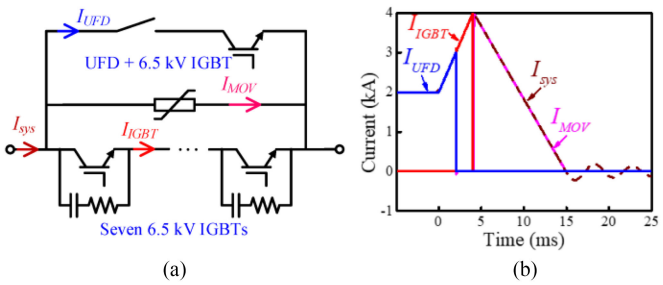

Fig. 8. (a) Topology, and (b) interrupting waveforms of the HCB.

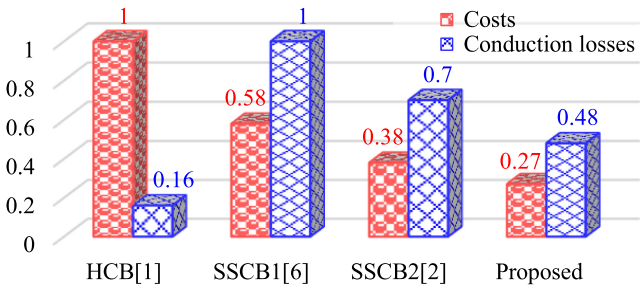

Fig. 9. Key characteristic comparison of four 25-kV/2-kA breakers.

TABLE II
COMPARISON OF DIFFERENT THYRISTOR-BASED SSCBS

Category	TBCB [9]	TFCB [11]	ΓSCB [3]	**Proposed**
Number of power devices	2n	6n	2n	**n**
Additional charging supply and/or strategies	YES	YES	NO	**NO**
Negative overvoltage problem caused by RRP	YES	YES	YES	**NO**
Interruption capability affected by outer circuit parameters	YES	NO	YES	**NO**

voltage. The clamping voltage of the MOV is set to 42 kV. The simulation results indicate that when compared with the IGBT-based SSCB, the MD-SSCB features a longer interrupting time mainly because the MD-SSCB needs additional time to recover its thyristors. However, the increased fault interrupting time only makes the fault current slightly larger than I_T, and thus has little impact on the reliability of the dc system. Furthermore, the designed 25-kV/2-kA MD-SSCB is compared with the HCB [1], the IGCT-based SSCB [2], and the IGBT-based SSCB [6] in the same power level. The relative costs and conduction losses are shown in Fig. 9. Here, IGCT (*5SHY35L4522*) is used. The ordinate is a relative value and "1" represents the maximum. It can be seen that when compared with other breakers, the MD-SSCB features the smallest costs while maintaining relatively low conduction losses. Considering costs and conduction losses together, the MD-SSCB is the optimal one among these breakers.

In order to further evaluate the advantages of the proposed solution, key features of four thyristor-based SSCBs are compared and summarized in Table II [3], [9], [11]. It can be seen that the MD-SSCB can utilize the fewest power devices to reliably interrupt faults without being affected by the negative overvoltage problem and the parameters of the outer circuit. As a result, when compared with existing breakers, the MD-SSCB has advantages of simpler structure, lower costs, higher power efficiency, and higher reliability.

IV. CONCLUSION

By combining the merits of IGBTs and thyristors, this letter proposes a novel MD-SSCB for MVdc and HVdc distribution systems. When compared with traditional solutions, the MD-SSCB has advantages of simpler structure, lower costs, higher power efficiency, and higher reliability, which makes the MD-SSCB a promising candidate for dc system protection. Detailed fault-interrupting principle and design guidelines of the MD-SSCB are presented. The feasibility of the proposed solution is validated by the experimental tests.

REFERENCES

[1] M. Callavik, A. Blomberg, J. Hafner, and B. Jacobson, "Break-through! ABB's hybrid HVDC breaker, an innovation breakthrough enabling reliable HVDC grids," *ABB Rev.,* vol. 2, pp. 7–13, Nov. 2012.
[2] Q. Lu *et al.*, "Design and analysis of a 375V/5kA solid-state DC circuit breaker based on IGCT," in *Proc. IEEE Int. Power Electron. Appl. Conf. Expo*, Shenzhen, China, pp. 1–5, Nov. 2018.
[3] Z. Zhou, J. Jiang, S. Ye, C. Liu, and D. Zhang, "A Γ-Source circuit breaker for DC microgrid protection," *IEEE Trans. Ind. Electron.*, vol. 68, no. 3, pp. 2310–2320, Mar. 2021.
[4] X. Zhang *et al.*, "A state-of-the-art 500-kV hybrid circuit breaker for a dc grid: The world's largest capacity high-voltage DC circuit breaker," *IEEE Ind. Electron. Mag.*, vol. 14, no. 2, pp. 15–27, Feb. 2020.
[5] C. Peng, X. Song, A. Q. Huang, and I. Husain, "A medium-voltage hybrid DC circuit breaker—Part II: Ultrafast mechanical switch," *IEEE J. Emerg. Sel. Top. Power Electron.*, vol. 5, no. 1, pp. 289–296, Mar. 2017.
[6] R. Wang *et al.*, "Design of an IGBT-series-based solid-state circuit breaker for battery energy storage system terminal in solid-state transformer," in *Proc. 45th Annu. Conf. IEEE Ind. Electron. Soc.*, pp. 6677–6682, Oct. 2019.
[7] Z. J. Shen, G. Sabui, Z. Miao, and Z. Shuai, "Wide-bandgap solid-state circuit breakers for DC power systems: Device and circuit considerations," *IEEE Trans. Electron Devices*, vol. 62, no. 2, pp. 294–300, Feb. 2015.
[8] J. Liu *et al.*, "Ultra-low ON-State voltage IGCT for solid-state DC circuit breaker with single-switching attribute," *IEEE Trans. Power Electron.*, vol. 36, no. 3, pp. 3292–3303, Mar. 2021.
[9] W. Chen *et al.*, "Evaluation of CS-MCT in DC solid state circuit breaker (SSCB) applications," *IEEE Trans. Ind. Appl.*, vol. 54, no. 5, pp. 5465–5473, Oct. 2018.
[10] R. Sander, M. Suriyah, and T. Leibfried, "Characterization of a countercurrent injection based HVDC circuit breaker," *IEEE Trans. Power Electron.*, vol. 33, no. 4, pp. 2948–2956, Apr. 2018.
[11] Y. Guo, G. Wang, D. Zeng, H. Li, and C. Hong, "A thyristor full-bridge-based DC circuit breaker," *IEEE Trans. Power Electron.*, vol. 35, no. 1, pp. 1111–1123, Jan. 2020.
[12] D. Keshavarzi, T. Ghanbari, and E. Farjah, "A z-source based bidirectional dc circuit breaker with fault current limitation and interruption capabilities," *IEEE Trans. Power Electron.*, vol. 32, no. 9, pp. 6813–822, Sep. 2017.
[13] Z. Dongye, L. Qi, X. Cui, P. Liu, and F. Lu, "A new approach to model reverse recovery process of a thyristor for HVdc circuit breaker testing," *IEEE Trans. Power Electron.*, vol. 36, no. 2, pp. 1591–1601, Feb. 2021.
[14] F. Liu, W. Liu, X. Zha, H. Yang, and K. Feng, "Solid-state circuit breaker snubber design for transient overvoltage suppression at bus fault interruption in low-voltage DC microgrid," *IEEE Trans. Power Electron.*, vol. 32, no. 4, pp. 3007–3021, Apr. 2017.
[15] F. Liu, W. Liu, X. Zha, H. Yang, and K. Feng, "Solid-State circuit breaker snubber design for transient overvoltage suppression at bus fault interruption in low-voltage DC microgrid," *IEEE Trans. Power Electron.*, vol. 32, no. 4, pp. 3007–3021, Apr. 2017.